Accepted Manuscript

Transendothelial migration of human umbilical mesenchymal stem cells across uterine endothelial monolayers: Junctional dynamics and putative mechanisms

Neven A. Ebrahim, Lopa Leach

PII: S0143-4004(16)30567-7

DOI: 10.1016/j.placenta.2016.10.014

Reference: YPLAC 3495

To appear in: *Placenta*

Received Date: 8 July 2016

Revised Date: 19 October 2016

Accepted Date: 20 October 2016

Please cite this article as: Ebrahim NA, Leach L, Transendothelial migration of human umbilical mesenchymal stem cells across uterine endothelial monolayers: Junctional dynamics and putative mechanisms, *Placenta* (2016), doi: 10.1016/j.placenta.2016.10.014.

Transendothelial migration of Human Umbilical Mesenchymal Stem Cells across uterine endothelial monolayers: junctional dynamics and putative mechanisms.

Neven A. Ebrahim and Lopa Leach*

Molecular Cell Biology & Development Group, School of Life Sciences, Faculty of Medicine & Health Sciences, University of Nottingham, Nottingham, UK. mbxnz1@nottingham.ac.uk; lopa.leach@nottingham.ac.uk

*Corresponding Author. School of Life Sciences, E Floor Medical School, Queens Medical Centre, Nottingham, NG7 2UH, UK. Email address: lopa.leach@nottingham.ac.uk. Tel +44 115 8230175; Fax +44 1158230142

Abbreviations: Mesenchymal stem cells (MSC) from Wharton's jelly of human umbilical cords (WJ-MSC), human uterine microvascular endothelial cells (HUtMEC), vascular endothelial cadherin (VE-cadherin), vascular endothelial growth factor (VEGF), cytokeratin 7 (CK-7), human umbilical vein endothelial cells (HUVEC).

Abstract

Introduction: During pregnancy, fetal stem cells can transfer to the maternal circulation and participate in tissue repair. How they transmigrate across maternal endothelial barriers and whether they can subsequently influence maternal endothelial integrity is not known.

Methods: Mesenchymal stem cells (WJ-MSC) were isolated from Wharton's jelly and their interactions with human uterine microvascular endothelial cell (HUtMEC) monolayers, junctional occupancy and expression /phosphorylation of vascular endothelial (VE)- cadherin and vascular endothelial growth factor (VEGF-A) secretion was studied over 48h by real time, confocal microscopy, immunoblotting and ELISA.

Results: WJ-MSC displayed exploratory behaviour with interrogation of paracellular openings and spreading into the resultant increased gaps followed by closing of the endothelium over the WJ-MSC. 62% of added cells crossed within 22h to sub-endothelial niches . There was a concomitant loss of junctional VE-cadherin in HUtMEC followed by a full return and increased VE-cadherin expression after 22h. During early hours, VE-cadherin showed a transient phosphorylation at Tyrosine (Tyr)-685 when VEGF-A secretion were high. From 16 to 22h, there was increased de-phosphorylation of Tyr-731. Anti-VEGF-A blocked Tyr-685 phosphorylation but not the decrease in P-Tyr731; this partially inhibited WJ-MSC transmigration.

Discussion: Fetal WJ-MSC can traverse uterine endothelial monolayers by mediating a non-destructive paracellular pathway. They can promote junctional stability of uterine endothelium from the sub-endothelial niche. Mechanistically, WJ-MSC induces VEGF-dependent phosphorylation events linked with paracellular permeability and VEGF-independent de-phosphorylation events associated with leukocyte extravasation. Our data also allows consideration of a possible role of fetal MSC in mature functioning of the uterine vasculature needed for optimal utero-placental perfusion.

Key words: Human umbilical mesenchymal stem cells, Human uterine microvascular endothelial cells, Transendothelial migration, VE-cadherin, P-Tyr685, P-Tyr731.

Introduction

The presence of pregnancy-associated fetal progenitor cells in the maternal circulation is well documented. They can be detected in the mother's peripheral blood from the first trimester of pregnancy, with numbers increasing as pregnancy progresses; indeed persistent microchimeric fetal cells can remain in the maternal circulation decades after birth [1-3]. The maternal blood in placental intervillous spaces has been shown to contain fetal cells even at term, strengthening the observation that these cells continue to cross the placental barrier throughout gestation [4]. Cells from all three embryonic germ layers; ectoderm, endoderm and mesoderm have been identified in maternal peripheral blood and damaged maternal tissues such as brain, kidney and heart [5-9]. They are thought to play an active role in the repair of maternal tissues; caudal related homeobox 2 (*CDX2)* cells of fetal/placental origin have been shown to home into injured myocardial endothelium in mice and undergo differentiation into diverse cardiac lineages [10]. The re-modelling of uterine spiral arteries up to one-third of the myometrium by placenta derived extra-villous trophoblast cells (EVT) in order to ensure high flow, low resistance conduits of maternal blood flow to the placenta is well documented [11]. EVT are thought to replace the smooth muscle layer of the arteries, with subsequent re-endothelisation or trans-differentiation to endothelial cells. Whether fetal mesenchymal stem cells could play a part in this has not been addressed. Other cell types, specifically fetal endothelial colony forming cells isolated from human cord blood and injected into the fetal heart have been shown to transmigrate from the fetus to the uterus and home into and aid expansion of mouse uterine vessels in pregnancy [12]. These authors also located endothelial-associated fetal cells in the human myometrial microvessels at term and hypothesise that fetal stem cells play a role in influencing the necessary expansion of maternal vascular supply to the placenta. How fetal cells, whether endothelial colony- forming or mesenchymal stem cells, cross the maternal endothelial barrier, incorporate into the uterine vasculature and their influence, if any, on the endothelium requires investigation.

Mesenchymal stem cells (MSC) can be found in perivascular niches of the placenta and umbilical cord [13, 14]. They are of interest in regenerative medicine, given their potential to promote tissue regeneration [15] and enhance vascular barrier integrity [13, 16]. WJ-MSC can promote neovascularisation, re-endothelialisation and junctional integrity [13, 17]. In a previous study we have shown that WJ-MSC can cross the fetal human umbilical vein endothelial monolayers using a paracellular route, with full repair of vascular endothelial cadherin (VE-cadherin) junctions once a sub-endothelial niche has been reached [13]. Whether a similar non-destructive mechanism is

employed by these fetal stem cells to cross the maternal endothelium, including the uterine myometrial microvascular endothelium require elucidation.

The endothelial paracellular pathway, and the adhesion molecules present therein respond to physiological and pathological factors including inflammatory mediators and permeability increasing agents such as VEGF and histamine [18-20]. Activation of Src family kinases and tyrosine phosphorylation of VE-cadherin has been associated with a loss of barrier function. VEGF has been shown to increase phosphorylation of Tyr-685 in human umbilical vein cells [19, 21]. However controversy exists in the literature, with Adam *et al.* [22] showing that Src-induced tyrosine phosphorylation of VE-cadherin is not sufficient to promote an increase in monolayer permeability in human dermal microvascular cells. A recent *in vivo* study suggests that the opening of endothelial junctions for the passage of plasma proteins or leukocytes depends on two different tyrosine residues of VE-cadherin where phosphorylation is regulated in opposite ways. Using knock-in mice expressing a Y685 mutant of VE-cadherin or a Y731F mutant, the authors demonstrated phosphorylation and dephosphorylation of VE-cadherin at Tyr685 and Tyr731 governs induction of vascular permeability or leukocyte diapedesis [23]. The latter required internalisation of VE-cadherin via tyrosine phosphatase SHP-2 with the resultant frank opening necessary for leukocyte paracellular trafficking. Which pathway, or both is utilised by WJ-MSC needs addressing. MSc derived from bone marrow have been shown to cross primary human lung and heart microvascular endothelial monolayers [24] in a fashion similar to leukocytes, although the duration of the process: from encounter to sub-endothelial destination, took longer than that for leukocytes crossing at sites of inflammation [13, 19, 24, 25].

Using real time, confocal microscopy, ELISA and protein expression analyses this study specifically investigated the spatio-temporal events when fetal WJ-MSC encounter confluent maternal endothelial cell monolayers, the chosen transendothelial migration pathway and the VE-cadherin dynamics and phosphorylation events which would allow physiological paracellular extravasation. The ability of these cells to influence maternal endothelial junctional maturity from sub-endothelial niches was also investigated. The use of primary uterine microvascular cells allowed insights to fetal and maternal interactions per se as well as a possible role of fetal mesenchymal stem cells in mature functioning of the uterine vasculature needed for optimal utero-placental perfusion.

Materials and Methods

Tissue Collection and Ethical Approval

Term umbilical cords (n=8) were obtained at elective Caesarean section from normal pregnancies with informed patient consent and full ethical approval (REC Ref 14/SC/ 1194; NHS Heath Research Authority, UK). The work described here has been carried out in accordance with The Code of Ethics of the World Medical Association (Declaration of Helsinki).

5 separate isolates of primary human uterine myometrial microvascular endothelial cells (C-12295; Passage 2) were bought from PromoCell, Heidelberg, Germany.

Antibodies used (concentration, clone and company): CD45 – FITC (0.25 µg/ml, Clone IM2078U, Beckman Coulter); CD34 – FITC (0.25 µg/ml, A86354, Beckman Coulter); CD44 – PE (0.25 µg/ml, IM0845, Beckman Coulter); CD29 – FITC (0.25 µg/ml PN IM0791U, Beckman Coulter); CD105 – FITC (0.25 µg/ml, 323203,ebioscience); CD73 – APC (0.125 µg/ml, 17-0739, ebioscience); CD90 – PE (0.25 µg/ml, 12-0909, ebioscience); CDHLA-DR – FITC (0.25 µg/ml, 307603,ebioscience); CD19 – APC (0.25 µg/ml, 12-0199, ebioscience); CD14 – PE (0.25 µg/ml, 17-0149, ebioscience); VE-cadherin (CD144; 5 µg/ml; 2500,Cell Signalling, UK); VE-cadherin (6 µg/ml, 55-7H1, Pharmingen, BD Biosciences); Vwf (5 µg/ml, IS527,Dako); CD31(5 µg/ml, BBA7, R&D Systems); Cytokeratin 7(12.4 µg/ml; M7018,Dako); VE-cadherin p-Tyr 685 (2 µg/ml, CP1981, ECM Biosciences); VE-cadherin p-Tyr731 (2 µg/ml, Ab27776, abcam); β-Actin (0.4 µg/ml, A5316, Sigma-Aldrich); VEGF-A (2 µg/ml, MAB293, R&D Systems); IgG secondary antibodies for IB (1:4000, Li-Cor Bioscience).

Isolation and characterization of cells

WJ-MSC were non-enzymatically isolated from umbilical cord segments and cultured up to Passage 4 in stem cell growth medium (DMEM/Low Glucose) with 0.1% antibiotic/antimycotic solution and 15 % Fetal Bovine Serum using the methods previously described [13]. They were characterised to be mesenchymal stem cells by flow cytometry, being positive for mesenchymal CD29, CD105, CD90, CD73, CD44 and negative for the haematopoetic markers CD34, CDHLA-DR, CD14, CD19 & CD45. The ability of these cells to differentiate into osteocytes, chondrocytes and adipocytes if induced was also tested separately [13]. Undifferentiated WJ-MSC were labelled

with the red fluorescent dye PKH26 (15 µM; Sigma-Aldrich, UK) as per manufacture's instruction prior to co-culture studies.

HUtMEC on 1 % gelatin-coated coverslips were grown to confluence in endothelial growth medium (MV) from PromoCell which contained 5.56 mM glucose, *FCS, ECGS, heparin, hydrocortisone but no extra VEGF;* pH 7.4. 100 IU/mL penicillin, 100 µg/mL streptomycin, 0.25 µg/mL Amphotercin B was added to MV before use. HUtMEC and WJ-MSC monolayers and co-cultures (see below) were further characterized by immunocytochemistry with antibodies against the endothelial markers VE-cadherin and CD31; mesenchymal marker CD29-FITC, anti-VEGF-A and mAb against cytokeratin 7 (Dako, UK). Rabbit-anti human VE-cadherin was used for double labelling. HUVEC monolayers at passage 2 were used as a positive endothelial control. Briefly, cells were fixed with 1% paraformaldehyde, permeabilized (0.15% Triton X-100; 10 min), blocked in 5% goat serum and incubated overnight (4 ˚C) with the primary antibodies. Appropriate TRITC or FITC conjugated secondary antibodies (Sigma) were then used. Coverslips were mounted using Vectorshield (Vector Lab Inc, USA). Propidium iodide (PI; 1.5µg/ml) or 4'6-diamidino-2-phenyl indole (DAPI; 1µg/ml) was used to counterstain nuclei. Images were acquired with Nikon fluorescence microscope and NIS elements F3.0.

Co-culture studies of WJ-MSC with HUtMEC

Similar to our previous study design using HUVEC [13], once HUtMEC reached 70 ⁒ confluence, media was changed to a 50:50 mixed media (endothelial: stem cell media). On full confluence (18 -24h later) isolated PKH26 labelled WJ-MSC were seeded on top of the confluent monolayer (1: 5 ratio) per coverslip [13, 16]. HUtMEC monolayers without added WJ-MSC acted as controls. All experiments were repeated 4 times.

Real Time Observations

Co-cultures of WJ-MSC with HUtMEC on gelatinized glass-bottomed tissue culture dishes (Ibidi GmBH, Germany) were observed for 24 hours with a wide-field fluorescence imaging system (Deltavision Elite; Applied Precision, USA). Z- stack images at 2 different focal planes were acquired every 15 min. Data analysis was carried out using Volocity software (Perkin Elmer, UK).

Quantitative analysis of endothelial junctional integrity and migrating WJ-MSC

Based on preliminary observations of co-cultures from 0- 48h, and known behaviour of WJ-MSC on HUVEC monolayers [13], confluent monolayers of HUtMEC with/without added PKH26-labelled WJ-MSC at 0, 30, 60, 90 min, 2, 16, 22 and 48 h were immunolabelled for VE-cadherin as stated above for analyses of early and late

interactions. Systematic random sampling was used to acquire 10 images per coverslip for each chosen duration and repeats. After blinding, the % of paracellular clefts per image was categorised according to VE-cadherin staining pattern: continuous or discontinuous (including total loss from cell-cell cleft). To ensure an equal chance of being counted, a grid was used and clefts from every other square which did not cross the "forbidden line" [27, 28] were counted. Data were analysed using Two-way ANOVA (Prism 6) and Sidak's multiple comparison test. Statistical significance was taken at $p<0.05$.

Using Z-focus steps, the location of WJ-MSC in respect to HUtMEC monolayer, whether above (apical) or below (sub-endothelial) and their proximity to discontinuous junctions were recorded at 30, 60, 90 min and 2, 16 and 22h.

Confocal imaging

2 and 22h immunostained coverslips were further analysed with confocal scanning microscopy (Zeiss Axiovision; Zeiss, Germany). Optical slices (0.5 - 0.6 µm intervals) were taken and composite images were tilted at the Z-axis with Volocity software to visualise transmigration pathways and the apical/basal location of stem cells for the chosen durations.

Immunoblot analysis

Confluent HUtMEC monolayers were co-cultured with/without unlabelled WJ-MSC on 6 well plates as above. Based on the observed VE-cadherin dynamics, the early hours of interaction (0, 30, 60 and 120 min) and late (22 and 48h) were chosen to measure VE-cadherin expression and its' phosphorylation status at Tyr-685 or Tyr-731. A third study group included co-cultures interacted in the presence of anti-human VEGF-A (2µg/ml) for 2 and 22h. Briefly, cells were scraped and lysed in 200 µl Lysis buffer (50 mM Tris-HCL pH 7.4; + 10 % [vol/vol] glycerol + 280 mM NaCl + 0.1% Triton X 100 + 50 mM NaF + 2 mM EGTA + 0.2 mM EDTA + 1 mM NA_3VO_4 + 0.1 mM phenylmethylsulfonyl fluoride [PMSF] + 1 mM Dithiothreitol (DTT) and Complete [Roche] protease inhibitors) for 10 min on ice. De-natured proteins were separated in a 4-20% gradient polyacrylamide gel (Bio-Rad, UK) after equal loading [13]. They were incubated with antibodies consecutively with immunoglobulins removed as described by Begitt et al [29]. Optical densities were measured and analysed using the Li-cor Odyssey system and Image-J. Normalised values, against β-actin and VE-cadherin were compared by One-way ANOVA and unpaired student's t-test [13]. Experiments were repeated three times using three different isolates.

ELISA Assay

VEGF-A (165 and 121) concentrations in the condition media from co-cultures of WJ-MSC and HUtMEC at 2, 22, 48h were measured using a commercially available kit (R&D Systems, USA). Conditioned media from co-cultures grown in the presence of neutralising anti-VEGF-A antibody were measured as was conditioned media from WJ-MSC or HUTMEC monolayers only. The optical absorbance was read at 450 nm (TECAN, Switzerland). VEGF-A concentrations were calculated from standard curves and analysed with One-way ANOVA. Internal repeats (x3) from two different isolates were compared.

Results

VE-cadherin junctional dynamics in co-cultures.

HUtMEC showed immunopositivity to the endothelial markers VE-cadherin and CD31 (Fig.1 A,B) with strong continuous staining at cell-cell contact regions of confluent monolayers. Counts of junctions in mixed media at different durations revealed a slight decrease in continuity after 30 min exposure to mixed media but this was not found to be statistically significant when compared to controls in full media. Values from subsequent 2h, 16h and 22h in mixed media were not statistically different from each other, 30 min duration or control (One way ANOVA with Tukeys Multiple Comparison test; Fig.1 C-G).

On addition of labelled WJ-MSC to confluent HUtMEC layers, WJ-MSC began to alter their shape, from rounded to more flattened cuboidal to elongated spindle shape with time. 30 min after initial interaction, 10% of cells displayed changed morphology (Fig 2 A); by 2h, <40% of cells remained rounded and could be found in apical positions only. (Fig 2 B). A contact-mediated change of VE-cadherin staining pattern in HUtMEC, from continuous to discontinuous or total loss, was observed from 30 min onwards (Fig.2 C, D). This reached statistical significance ($P < 0.0001$) at 2h with $63 \pm 4.6\%$ of clefts showing continuous staining compared to controls (83.5 ± 3.5 %). Disrupted clefts and frank openings at tri-cellular junctions in the monolayer were associated with overlying or transmigrating WJ-MSC (Fig. 2 C-E). At 16h co-culture there was evidence of recovery in regions devoid of apically resident stem cells; 79 ± 1.7 % of junctions now displayed continuous VE-cadherin. At 22h, WJ-MSC were found mostly in sub-endothelial position, underlying fully confluent endothelial monolayers with continuous VE-cadherin staining (Fig. 2 F). This was confirmed by the Z tilts acquired at 2 and 22h (Fig.2 G, H). At 22h, 94 ± 2.7 % of clefts showed continuous VE-cadherin staining compared to 82.2 ± 2.5 % in duration matched controls ($p <$

0.001) suggestive of increased junctional occupancy of VE-cadherin in the stem cell treated HUtMEC (Fig.2 I). WJ-MSC demonstrated negative immunoreactivity to VE-cadherin throughout.

Counts of PKH26 labelled WJ-MSC at apical, transmigrating or sub-endothelial locations confirmed that transmigration started from 30 minutes (5% of total cells in field of view) with the number of extravasating cells increasing with time (Fig. 2 J). The rate of migration was highest in the early hours, with 48 $\pm$ 15 % of cells found in sub-endothelial locations at 2h. Migration continued for a further twelve hours with 98 $\pm$ 2% of WJ-MSC counted at sub-endothelial positions at 22h. Not all cells crossed the endothelial barrier, of the initial 20,000 cells placed on confluent HUtMEC per coverslip, only 62 $\pm$ 18% of cells crossed within 22h.

Real time visualisation of WJ-MSC/ HUtMEC interactions

Real time microscopy confirmed that interaction with WJ-MSC did not result in any observed apoptosis or detachment of the uterine endothelial cells. HUtMEC remained as a flattened monolayer throughout the 48h observation period (Fig.3). Upon addition, the PKH26-labelled WJ-MSC displayed a prolonged exploratory behaviour, with classical membrane blebbing and amoeboid movement (Fig. 3 A-M) over the uterine endothelial monolayer. After the lag phase, WJ-MSC was observed to change shape towards the spindle-shaped morphology (Fig.3 N-P), interrogate endothelial paracellular clefts and populate the increased paracellular gaps in HUtMEC monolayers (Fig.3 N-R).

Analyses of VE-cadherin expression/ phosphorylation status

The expression and phosphorylation status of VE-cadherin was altered depending on presence and duration of stem cell interaction (Fig.4 A-E). In the early hours of co-culture, 0, 30, 60 and 120 min there were no change in the total expression of VE-cadherin. At the post-migration times of 22 and 48h co-culture, there was a statistically significant ($p< 0.01$) increase in VE-cadherin expression, compared to control or early hours (Fig. 4A, D).

HUtMEC treated with WJ-MSC showed a significant increase in p-Tyr685 at early hours (30, 60 and 120 min) reaching maximal value at 2h ($p<0.001$), followed by a decrease at 22h and return to control values at 48h (Fig.4 A, B). Tyr731 showed basal level of phosphorylation similar to the controls at the early hours of interaction (Fig.4 C). This was followed by a dramatic decrease in p-Tyr731 expression at 2 and 22h ($p<0.01$). By 48h, both phosphorylation and de- phosphorylation status of VE-cadherin returned to normal.

Addition of anti-VEGF neutralising antibodies to co-cultures blocked the phosphorylation of Tyr685 at 2 and 22h, with a significant decrease at 2h ($p<0.01$; Fig 4E). The later Tyr731 de- phosphorylation was not affected.

Neutralisation of VEGF resulted in reduced migration of WJ-MSC with 25% fewer cells found in sub-endothelial locations at 2h. Cells continued to cross the endothelial monolayer in the period dominated by the unaltered Tyr731 de-phosphorylation. At 22h, only 47 ± 6 % of cells, compared to 90 ± 8% in non-neutralised controls, were found underlying the HUtMEC monolayer (Fig. 4 F).

Secretion of VEGF during early hours of interaction

The conditioned media (CM) from WJ-MSC or HUtMEC monolayers showed negligible concentrations of VEGF-A (165,121) present (Fig.5 A). In cultures of HUtMEC challenged with mixed media there was a detectable level of VEGF-A levels in the supernatant measured at 2h but not at 22h. When HUtMEC was co-cultured with WJ-MSC there was a statistically significant increase in VEGF-A levels in the supernatant at 2h ($p<0.001$) followed by a decrease at 22h ($p<0.05$). No VEGF-A was detected by 48h. Supernatants of co-cultures grown in the presence of VEGF-A neutralising antibodies did not contain measurable VEGF-A at 2 or 22h. Immunocytochemistry revealed VEGF-A presence in HUtMEC and WJ-MSC (Fig.5 B-D). WJ-MSC appeared to have higher intensity of staining at 2h co-culture (Fig 5B).

Cytokeratin-7 expression in endothelial and mesenchymal stem cells

In monocultures, 29 ± 4% of HUtMEC were immunopositive to CK7 whilst still expressing endothelial markers (Fig.6 A,B); HUVEC were found to contain a higher percentage (81± 6%) of CK-7 expressing cells (Fig.6 C,D) whilst 30 ± 3% of the WJ-MSC were positive to CK7 (Fig.6 E) whilst also expressing mesenchymal markers (Fig.6 F). In HUtMEC-WJMSC co-cultures, no increase was seen in the percentage of CK7+ cells in either cell type (Fig.6 G, H). $CK7^+$ WJ-MSC was found in both apical and sub-endothelial positions of HUtMEC monolayers at 2 or 22h of co-culture.

Discussion

This *in vitro* study is the first to show that fetal mesenchymal stem cells derived from the Wharton's jelly of term human umbilical cords can cross monolayers of microvascular endothelial cells derived from the human myometrium in a non-destructive manner without detaching the endothelial cells of the monolayer. Moreover, these fetal mesenchymal cells demonstrated a paracellular egress to sub-endothelial niches with disruption of VE-cadherin junctions followed by repair and increased up-regulation of VE-cadherin. In the early hours of co-culture, WJ-MSC induced phosphorylation of the Tyr 685 residue of VE-cadherin which has been implicated in initiation of vascular permeability. This was followed by de-phosphorylation of Tyr731, implicated in regulation of leukocyte

extravasation. The early VE-cadherin discontinuity at cell-cell junctions and phosphorylation at Tyr685 may be induced by soluble factors secreted during co-culture. Elevated levels of VEGF were found in the supernatant prior to and during maximal rate of transendothelial migration of WJ-MSC. Both cell types were capable of secreting VEGF with WJ-MSC showing higher intensity of staining at 2h co-culture.

HUtMEC have been used previously to investigate trophoblast invasion and integration into the endothelial layers [30]. Trophoblast cells were shown to actively displace endothelial cells and form trophoblast islands in the same plane as the endothelial cells. WJ-MSC appeared not to displace HUtMEC but rather transmigrated singly to sub-endothelial regions. This behaviour was similar to that when WJ-MSC encountered fetal endothelial cells isolated from umbilical cords (13). Sipos *et al*. [12] demonstrated that human fetal endothelial colony forming cells can cross the placental feto-maternal barrier and transmigrate to the maternal uterine vasculature in mice. These cells exhibited mesenchymal markers (CD105 & CD 146) and endothelial markers (CD 31) and VEGFR-2, but not hematopoietic markers. In our study we demonstrate that fetal mesenchymal stem cells, isolated from cords obtained from elective Caesarean sections, can also traverse maternal endothelial cells and influence their junctional integrity once sub-endothelial locations are reached.

WJ-MSC displayed non-apoptotic blebbing, amoeboid movement and interrogation of intercellular openings (Fig. 3) as early events in their exploration of the uterine endothelial monolayer. This is reminiscent of bone marrow mesenchymal cell interactions with TNF- alpha stimulated endothelial cells [24]. There was a minimum time lag of around 30 min before WJ-MSC transmigration was observed with a higher rate of migration between 30 min to 2h. The differential rate of migration over the study period suggests to the presence of two populations: fast and slow transmigrators. Furthermore, only 60% of cells placed on the endothelial monolayers crossed suggesting that in our non-stimulated confluent monolayers, the microenvironment may have favoured cells capable of peri-vascular/pericytic commitment. The observed prolonged exploration shown by WJ-MSC and the induced paracellular gaps in HUtMEC monolayer suggests a paracrine conversation between WJ-MSC and the endothelial cells. Indeed, VEGF levels increased in co-culture supernatants at 30 min, with highest levels measured at 2h. MSC isolated from chorionic blood vessels of the placenta has been shown to secrete VEGF and induce increased angiogenesis in endothelial cells from chorionic arteries [31]. It is therefore not surprising that WJ-MSC, of same mesodermal origin also shows a similar secretory capability when challenged with HUtMEC. The highest percentage of junctional disruption, defined by loss or discontinuous VE-cadherin localisation was also recorded at

2h. The ability of VEGF to disrupt VE-cadherin junctions is well established [18, 20, 28]. Junctional VE-cadherin profiles returned to normal when a majority of WJ-MSC were resident underneath the endothelial monolayers. Indeed, at 22h there was increased monolayer integrity manifested by a significantly higher percentage of paracellular clefts showing continuous VE-cadherin labelling compared to HUtMEC monolayers without stem cells. The higher VE-cadherin protein expression at 22 and 48h also indicates an induced increase in junctional maturity. WJ-MSC were seen to expel exosomes (data not shown); the role of these in the subsequent upregulation of VE-cadherin is under investigation in our lab. Although our data is from *in vitro* studies, the observed non-destructive migration and post-migratory influence on junctional integrity of uterine endothelial cells is encouraging and offers possible mechanisms as to how fetal stem cells can traffic and reside in maternal tissue. Certainly, the data strengthens the promise of the usefulness of WJ-MSC in vascular repair of maternal/adult vasculature.

The molecular mechanism utilised by the fetal stem cells to cross the uterine endothelial barrier, appeared to involve transient phosphorylation of VE-cadherin at Tyr685. The resultant transmembrane redistribution of VE-cadherin from junctional regions may have allowed early egress of the spindle-shaped WJ-MSC. This was partially blocked by VEGF-A neutralising antibodies, which also inhibited phosphorylation of VE-cadherin. VEGF-A have been shown to target the Y685 residue of VE-cadherin [21]. Increased P-Y685 in our study coincided with increased VEGF-A measured at the early hours of co-culture. VEGF-A was immunolocalised to both HUtMEC and WJ-MSC, the latter showed higher intensity of staining at 2h. Of course, VEGF-A may only be one contributory secretory factor, given WJ-MSC can secrete a repertoire of permeability enhancing factors and cytokines which are also able to induce SRC-mediated VE-cadherin changes. Although we did not observe intracellular migration of the fetal stem cells, we cannot exclude this and it may also have contributed to why we only saw a partial inhibition of transmigration with neutralising antibodies against VEGF-A (25% reduction). As stated before, Wessel *et al* [19] showed that whilst Tyr685 phosphorylation induces vascular solute permeability, de-phosphorylation of VE-cadherin at Tyr731 selectively regulates leukocyte extravasation. In their study, siRNA blocking of the de-phosphorylation impaired VE-cadherin internalisation and reduced leukocyte migration by 36 %. In the WJ-MSC/HUtMEC co-cultures, the Y685 phosphorylation was followed by enhanced de- phosphorylation of Try731 at 2h; this coincided with highest recorded loss of junctional VE-cadherin and frank inter-cellular gaps. Addition of anti-VEGF antibody did not affect this de- phosphorylation suggesting VEGF independence. Overall our data suggests that a proportion of WJ-MSC may utilise pathways created by early VEGF-dependent VE-cadherin

331 perturbations at transmembrane domains, whilst the remainder may use the later VEGF-independent Tyr 731 de-
332 phosphorylation events that lead to internalisation of VE-cadherin and increased disruption of junctions. The two
333 putative mechanisms are also suggestive of the presence of at least two different sub-populations of WJ-MSC in our
334 isolated cultures.
335 Studies into the re-modelling of uterine spiral arteries have used cytokeratin-7 and karyotyping to conclude that
336 placenta derived extra-villous trophoblast cells invade and modify these maternal vessels. However, in our study
337 cytokeratin 7 (CK7) displayed a ubiquitous localisation in endothelial and human umbilical mesenchymal stem cells.
338 The percentage of WJ-MSC showing positivity to CK 7 may be related to a specific cohort in the isolated stem cells
339 or to a mesenchymal-epithelial transition of these cells in culture. However, this phenotype did not necessarily
340 promote transmigration of stem cells; they were found in apical and basal locations at both 2 and 22h. A recent
341 study demonstrated the heterogeneity and intrinsic potential of WJ-MSC to express epithelial markers including CK
342 7 in situ and in culture conditions [32]. Indeed, human bone marrow mesenchymal stem cells have been induced to
343 express CK 7 [33], whilst a percentage of stem cells from the human amnion have also been shown to express CK 7
344 *in situ* [34]. The endothelial localisation we found in HUVEC was curious; the co-expression of cytokeratin 7 and
345 VE-cadherin (Fig 6) confirmed their endothelial phenotype but suggested a de-differentiation capability of fetal
346 endothelial in conditions that favour proliferation and migration. The persistence of CK7 positive cells in the
347 HUtMEC suggests this is not just a fetal trait. Moster *et al*. [35] suggested that anti-CK 7 alone is not adequate to
348 distinguish between different trophoblast subtypes. Our studies further strengthen the concept that multiple markers
349 need to be used when deciding trophoblast origin of fetal cells found in maternal spiral arteries.
350 Whilst fetal mesenchymal stem cells have been identified in maternal peripheral blood and damaged maternal
351 tissues [9,10], how they cross the placental syncytiotrohoblast barrier into maternal intervillous blood lakes in the
352 first instance remain unexplained. In the first trimester, mesenchymal stem cells invading the umbilical and villous
353 cores may be able to migrate through cytotrophoblast cell shells or columns. One could speculate that during
354 gestation, chorionic villous regions, denuded of syncytiotrophoblast, may allow opportunistic escape of villous
355 MSC. Furthermore, transient inflammatory/pressure events during pregnancy may cause breaches or induce
356 transtrophoblastic channels in the syncytiotrophoblast; Kertschanska & Kaufmann presented morphological
357 evidence of this in the 1990s and showed experimentally that they could be induced during fetal perfusion of human
358 placental villi [36, 37]. Physiologically, villous MSC who are the nearest neighbours may be the ones that could

migrate during pregnancy, although this requires experimental demonstration and is beyond the remit of this paper. Regardless of anatomical location of isolated MSC from the extra-embryonic tissue, the ability of fetal MSC to interact with and influence uterine endothelial cells opens new avenues of enquiry regarding feto-maternal cross talk.

In conclusion, the data obtained in this study addresses an important question as to how fetal stem cells cross the maternal endothelium. Moreover, the transit times for MSC transendothelial migration and the mechanisms employed may be valuable for stem cell cytotherapy. Our data also opens a debate into how uterine spiral arteries are remodelled in pregnancy and whether other fetal stem cells, especially ones which can display non-destructive transendothelial migration and endothelial junctional repair may also be involved. Finally, the perivascular support function shown by WJ-MSC both to fetal and adult endothelial cells increases the potential usefulness of these extra-embryonic stem cells.

Acknowledgment

The DeltaVision Microscope used was funded by Wellcome Trust, 094233/Z/10/Z. The research was funded by the PhD programme at the University of Nottingham. We wish to thank Year 3 medical students Jennifer Sedcole and Olivia Volk for their help with the counts of cell migration at the early time points.

Disclosure Statement

The authors have no conflict of interest.

References

[1]. Dawe GS, Tan XW, and Xiao ZC. (2007). Cell migration from baby to mother. Cell Adh Migr 1:19-27.

[2]. O'Donoghue K., Choolani M., Chan J., de la Fuente J., Kumar S., Campagnoli C., Bennett P.R., Roberts I.A., and Fisk N.M. (2003). Identification of fetal mesenchymal stem cells in maternal blood: implications for non-invasive prenatal diagnosis. Mol Hum Reprod 9:497-502.

[3]. Bianchi DW. (2004). Fetomaternal cell traffic, pregnancy-associated progenitor cells, and autoimmune disease. Best Pract Res Clin Obstet Gynaecol 18:959-975.

[4]. Parant O, Dubernard G, Challier JC, Oster M, Uzan S, Aractingi S, and Khosrotehrani K. (2009). CD34+ cells in maternal placental blood are mainly fetal in origin and express endothelial markers. Lab Invest 89:915-923.

[5]. Seppanen E, Fisk NM, and Khosrotehrani K. (2013). Pregnancy-acquired fetal progenitor cells. J Rep Immunol 97:27-35.

[6]. Seppanen EJ, Hodgson SS, Khosrotehrani K, Bou-Gharios G, and Fisk NM. (2012). Fetal microchimeric cells in a fetus-treats-its-mother paradigm do not contribute to dystrophin production in serially parous mdx females. Stem Cells Dev 21:2809-2816.

[7]. Zeng XX, Tan KH, Yeo A, Sasajala P, Tan X, Xiao ZC, Dawe G, and Udolph G. (2010). Pregnancy-associated progenitor cells differentiate and mature into neurons in the maternal brain. Stem Cells Dev 19:1819-1830.

[8]. Cha D., Khosrotehrani K, Kim,Y, Stroh H, Bianchi DW, and Johnson KL. (2003). Cervical cancer and microchimerism. Obstet Gynecol 102:774-781.

[9]. Roy E, Seppanen E, Ellis R, Lee ES, Khosrotehrani K, Fisk NM, and Bou-Gharios G. (2014). Biphasic recruitment of microchimeric fetal mesenchymal cells in fibrosis following acute kidney injury. Kidney Int. 85:600-610.

[10]. Kara RJ, Bolli P, Karakikes I, Matsunaga I, Tripodi J, Tanweer O, Altman P, Shachter NS, Nakano A, and Najfeld V. (2012). Fetal cells traffic to injured maternal myocardium and undergo cardiac differentiation. Circ Res 110:82-93.

[11]. Pijnenborg R, Vercruysse L, and Brosens I. (2011). Deep placentation. Best Pract Res Clin Obstet Gynaecol 25:273-285.

[12]. Sipos PI, Rens W, Schlecht H, Fan X, Wareing M, Hayward C, Hubel CA, Bourque S, Baker PN, and Davidge ST. (2013). Uterine vasculature remodeling in human pregnancy involves functional macrochimerism by endothelial colony forming cells of fetal origin. Stem Cells 31:1363-1370.

[13]. Ebrahim NA, and Leach L (2015). Temporal studies into attachment, VE-cadherin perturbation, and paracellular migration of human umbilical mesenchymal stem cells across umbilical vein endothelial monolayers. Stem Cells Dev 24:426-436.

[14]. Castrechini NM, Murthi P, Gude NM, Erwich JJ, Gronthos S, Zannettino A, Brennecke SP, and Kalionis B. (2010). Mesenchymal stem cells in human placental chorionic villi reside in a vascular Niche. Placenta 31:203-212.

[15]. Uccelli A, Laroni A, and Freedman MS. (2011). Mesenchymal stem cells for the treatment of multiple sclerosis and other neurological diseases. Lancet Neurol 10:649-656.

[16]. Pati S, Khakoo AY, Zhao J, Jimenez F, Gerber MH, Harting M, Redell JB, Grill R, Matsuo Y, and Guha S. (2011). Human mesenchymal stem cells inhibit vascular permeability by modulating vascular endothelial cadherin/beta-catenin signaling. Stem Cells Dev 20:89-101.

[17]. Aguilera V, Briceno L, Contreras H, Lamperti L, Sepulveda E, Diaz-Perez F, Leon M, Veas C, Maura R, and Toledo JR. (2014). Endothelium trans differentiated from Wharton's jelly mesenchymal cells promote tissue regeneration: potential role of soluble pro-angiogenic factors. PloS one 9:e111025.

[18]. Esser S, Lampugnani MG, Corada M, Dejana E, and Risau W. (1998). Vascular endothelial growth factor induces VE-cadherin tyrosine phosphorylation in endothelial cells. J Cell Sci 111 (Pt 13):1853-1865.

[19]. Wessel F., Winderlich M, Holm M, Frye M, Rivera-Galdos R, Vockel M, Linnepe R, Ipe U, Stadtmann A, and Zarbock A. (2014). Leukocyte extravasation and vascular permeability are each controlled in vivo by different tyrosine residues of VE-cadherin. Nat Immunol 15:223-230.

[20]. Dejana E, Orsenigo F, and Lampugnani MG. (2008). The role of adherens junctions and VE-cadherin in the control of vascular permeability. J Cell Sci 121:2115-2122.

[21]. Wallez Y, Cand F, Cruzalegui F, Wernstedt C, Souchelnytskyi S, Vilgrain I, and Huber P. (2007). Src kinase phosphorylates vascular endothelial-cadherin in response to vascular endothelial growth factor: identification of tyrosine 685 as the unique target site. Oncogene 26:1067-1077.

[22]. Adam AP, Sharenko AL, Pumiglia K, and Vincent PA. (2010). Src-induced tyrosine phosphorylation of VE-cadherin is not sufficient to decrease barrier function of endothelial monolayers. J Biol Chem 285:7045-7055.

[23]. Sidibe A, and Imhof BA (2014). VE-cadherin phosphorylation decides: vascular permeability or diapedesis. Nat Immunol 15:215-217.

[24]. Teo GS, Ankrum JA, Martinelli R, Boetto SE, Simms K, Sciuto TE, Dvorak AM, Karp JM, and Carman CV. (2012). Mesenchymal stem cells transmigrate between and directly through tumor necrosis factor-alpha-activated endothelial cells via both leukocyte-like and novel mechanisms. Stem Cells 30:2472-2486.

[25]. Stock C, and Riethmuller C (2011). Endothelial activation drives lateral migration and diapedesis of leukocytes. Cell Immunol 271:180-183.

[26]. Dominici M, Le Blanc K, Mueller I, Slaper-Cortenbach I, Marini F, Krause D, Deans R, Keating A, Prockop D, and Horwitz E. (2006). Minimal criteria for defining multipotent mesenchymal stromal cells. The International Society for Cellular Therapy position statement. Cytotherapy 8:315-317.

[27]. Gundersen HJ, and Jensen EB (1987). The efficiency of systematic sampling in stereology and its prediction. J Microsc 147:229-263.

[28]. Leach L, Gray C, Staton S, Babawale MO, Gruchy A, Foster C, Mayhew TM, and James DK. (2004). Vascular endothelial cadherin and beta-catenin in human fetoplacental vessels of pregnancies complicated by Type 1 diabetes: associations with angiogenesis and perturbed barrier function. Diabetologia 47:695-709.

[29]. Begitt, A., Droescher, M., Meyer, T., Schmid, C.D., Baker, M., Antunes, F., Knobeloch, K.P., Owen, M.R., Naumann, R., Decker, T., et al. (2014). STAT1-cooperative DNA binding distinguishes type 1 from type 2 interferon signaling. Nature Immunol 15, 168-176.

[30]. Bainbridge SA, Roberts JM, von Versen-Hoynck F, Koch J, Edmunds L, and Hubel CA. (2009). Uric acid attenuates trophoblast invasion and integration into endothelial cell monolayers. Am J Physiol Cell Physiol 297:C440-450.

[31]. König J[1], Weiss G, Rossi D, Wankhammer K, Reinisch A, Kinzer M, Huppertz B, Pfeiffer D, Parolini O, Lang I. (2015). Placental mesenchymal stromal cells derived from blood vessels or avascular tissues: what is the better choice to support endothelial cell function? Stem Cells Dev. 24(1):115-31.

[32]. Garzon I, Alfonso-Rodriguez CA, Martinez-Gomez C, Carriel V, Martin-Piedra MA, Fernandez-Valades R, Sanchez-Quevedo MC, and Alaminos M. (2014). Expression of epithelial markers by human umbilical cord stem cells. A topographical analysis. Placenta 35:994-1000.

[33]. Tian H, Bharadwaj S, Liu Y, Ma PX, Atala A, and Zhang Y. (2010). Differentiation of human bone marrow mesenchymal stem cells into bladder cells: potential for urological tissue engineering. Tissue Eng Part A 16:1769-1779.

[34]. König J1, Lang I, Siwetz M, Fröhlich J, Huppertz B. (2014). Amnion-derived mesenchymal stromal cells show a mesenchymal-epithelial phenotype in culture. Cell Tissue Bank. 15(2):193-8.

[35]. Moser G, Orendi K, Gauster M, Siwetz M, Helige C, and Huppertz B. (2011). The art of identification of extravillous trophoblast. Placenta 32:197-199.

[36]. Kertschanska S, Kodanke G, Kaufmann P. (1994). Is there morphological evidence for the existence of transtrophoblastic channels in human placental villi? Trophoblast Research 8:581-596.

[37] Kertschanska S, Kodanke G, Kaufmann P. (1997). Pressure dependence of so-called transtrophoblastic channels during fetal perfusion of human placental villi. Microsc Res Tech 38:52-62.

Figure legends

Fig 1. Immunofluorescence analysis of HUtMEC grown in endothelial medium (A,B) and mixed media (C-F). (A). VE-cadherin show a predominant continuous staining pattern at cell-cell borders although some disruptions (arrow) are present; nuclei stained with PI. (B). HUtMEC also express CD31 at cell-cell boundaries; nuclei stained with DAPI. (C -F). VE-cadherin staining pattern in mixed media for 30 min, 2, 16 and 22h. Arrows point to discontinuous VE-Cadherin staining. (G) Graph showing % of continuous staining at different durations compared to control. Scale bar = 50 µm.

Fig 2. Spatio-temporal analyses of junctional VE-cadherin and WJ-MSC transmigration.
A to F are co-culture images taken from coverslips inverted on microscope slides; Z focus on VE-cadherin (green) staining of HUtMEC. Bar = 50 µm. (A) Apically resident PKH26 labelled WJ-MSC (red) showing rounded morphology and close association with overlying HUtMEC cell-cell boundaries at 30 minutes. (B) Micrograph showing a rounded WJ-MSC overlying HUtMEC and a spindle-shaped WJ-MSC (arrow) under a disrupted junction at 2h. (C, D) Increased number of cell-cell junctions with VE-Cadherin discontinuity or total loss of staining (arrows) can be seen in HUtMEC, 2 hours after addition of WJ-MSC. (E) At 16h, more WJ-MSC (*) can now be

493 seen underlying HUtMEC. Arrow points to a WJ-MSC traversing the endothelial layer across a disrupted border.
494 (F). At 22h, majority of junctions demonstrate continuous VE-Cadherin staining including those associated with
495 basal WJ-MSC. (G). Z-tilt of VE-cadherin stained confocal images after 2h co-culture. WJ-MSC show paracellular,
496 apical (a) and basal (b) location. (H). Z-tilt at 22h showing predominantly basal (sub-endothelial) location of WJ-
497 MSC. Bar = 100 µm. (I) Graph showing % of continuous VE-cadherin junctions at different duration of co-culture.
498 Two-way ANOVA showed a decrease at 2 h ($P < 0.0001$) and increase at 22 h ($P < 0.001$). (J) Graph showing the
499 increasing percentage of total WJ-MSC found in sub-endothelial position with time.
500
501 Fig. 3. Time lapse images of WJ-MSC on HUtMEC monolayer.
502 Micrographs showing sequential (every 15') acquisitions with Z focus on the PKH26 labelled WJ-MSC (red) taken
503 from 30 min after addition. (A-M) A rounded stem cell (*) can be seen displaying membrane blebbing as it moves
504 on HUtMEC monolayer towards a paracellular cleft. (N) The cell can be now be seen to change its rounded shape
505 to a more spindle-shape morphology and has psuedopodial extensions. 2 other stem cells (1, 2) which could be seen
506 out of plane of focus from Fig E are now in the same plane of focus in the cleft having moved to the same
507 paracellular cleft. (O) The starred cell (*) now has a more elongated morphology and jostles for space in the
508 paracellular cleft with the elongated spindle shaped cell 1 and intermediate shaped cell 2 (P,Q,R) . Bar = 14 µm.
509
510 Fig. 4. Immunoblot analyses of VE-cadherin, p-Tyr685 and p-Tyr731.
511 (A) Immunoblots of HUtMEC co-cultured with (C0-C48h), without WJ-MSC (E0-E22h) and co-cultures in the
512 presence of anti-VEGF (A2h & A22h). β-actin acted as loading control. (B). Graph showing statistically significant
513 increase in p-Tyr685/VE-cadherin at 0.5, 1, 2h and decrease at 22h and 48h (to normal basal level) in co-cultures.
514 (C) Tyr731 shows a basal level of phosphorylation similar to the controls at 0, 0.5 and 1h, followed by a decrease in
515 p-Tyr731 expression at 2h ($p<0.001$) and 22h ($p<0.01$). By 48h, phosphorylation status of p-Tyr is similar to normal.
516 (D) Graph showing VE-cadherin upregulation at 48h ($p<0.01$). (E) Graph showing effect of neutralising anti-VEGF
517 on p-Tyr685 at 2 & 22h ($p<0.01$). (F). Fluorescent micrograph of 22h co-culture grown in presence of anti-VEGF.
518 Numerous WJ-MSC can be seen in both apical and basal (*) locations. Bar = 50 µm.
519
520 Fig. 5. A. VEGF-A concentrations in conditioned media (CM) at different durations.

ELISA revealed negligible concentrations in WJ-MSC CM. A detectable level was found in HUtMEC CM. HUtMEC grown in mixed media showed an increase at 2h which became undetectable at 22 and 48h. Addition of WJ-MSC resulted in increased VEGF-A at 2h ($p < 0.001$) followed by a decrease ($p < 0.1$) at 22h. No VEGF-A was detected by 48h. VEGF-A was undetectable in co-cultures grown in the presence of VEGF-A neutralising antibodies. (Fig 5 B-D). Immunofluorescence images showing cytoplasmic localisation of VEGF-A (green) in HUTMEC and PKH26 (red) labelled WJ-MSC co-cultures. WJMSC show a higher intensity of staining at 2h (B); decreased intensity of staining was seen in both cell types by 48h (D). (E) Control image without primary antibody. No VEGF (green) staining can be seen in HUtMEC or PKH26 (red) labelled WJ-MSC. Bar = 50 µm.

Fig 6. Cytokeratin-7 expression in endothelial and mesenchymal stem cells

(A) VE-cadherin (red) positive HUtMEC monolayer showing CK-7 intermediate filaments (green) in a proportion of cells. (B) A second source of HUtMEC showing the presence of VE-cadherin+ (now double labelled with FITC; green) and CK-7+ (red; TRITC) cells; nuclei – DAPI. (C & D) HUVEC cells showing dual positivity to VE-cadherin (red) at cell-cell borders and CK-7 filaments (green). (E) WJ-MSC monoculture showing immunonegativity to VE-cadherin (red) with a few cells demonstrating filamentous CK-7 green staining; nuclei-DAPI. (F) WJ-MSC monolayers immunolabelled with CK-7 (red) & the mesenchymal marker CD29 (green). A cohort of CD29+ cells show co-localisation with CK-7 (yellow). (G) PKH26 labelled WJ-MSC (w) on HUtMEC showing CK-7 expression (green) at 2h. (H) Sub-endothelial WJ-MSC (w) at 22h. Both CK-7 positive (green) and negative (red) cells can be seen. Bar = 50 µm.

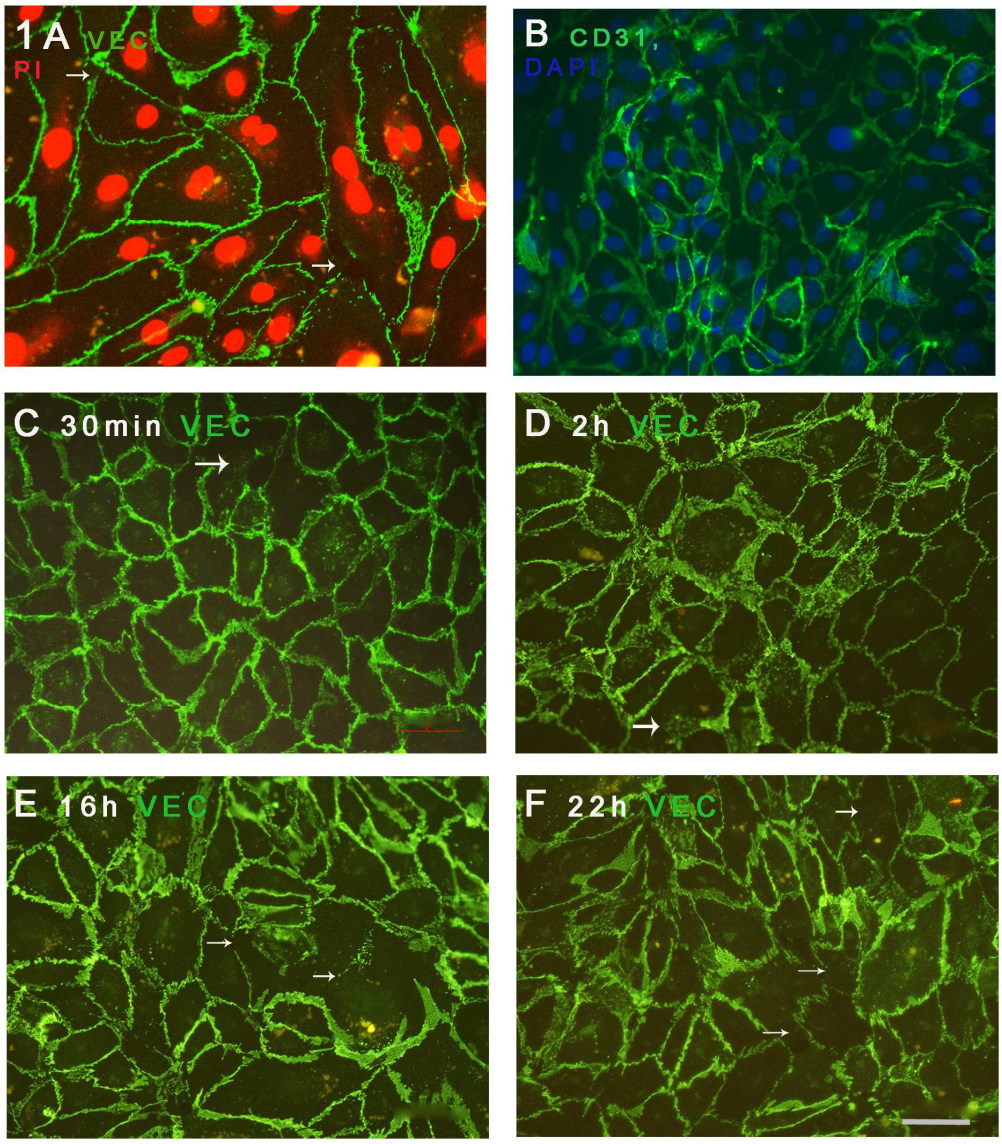

G Effect of mixed media on junctional VE-cadherin

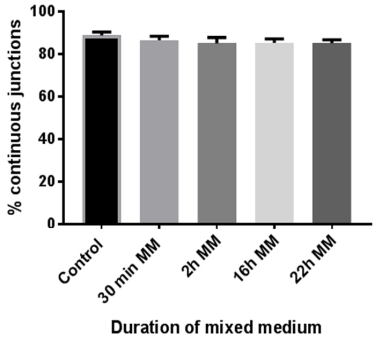

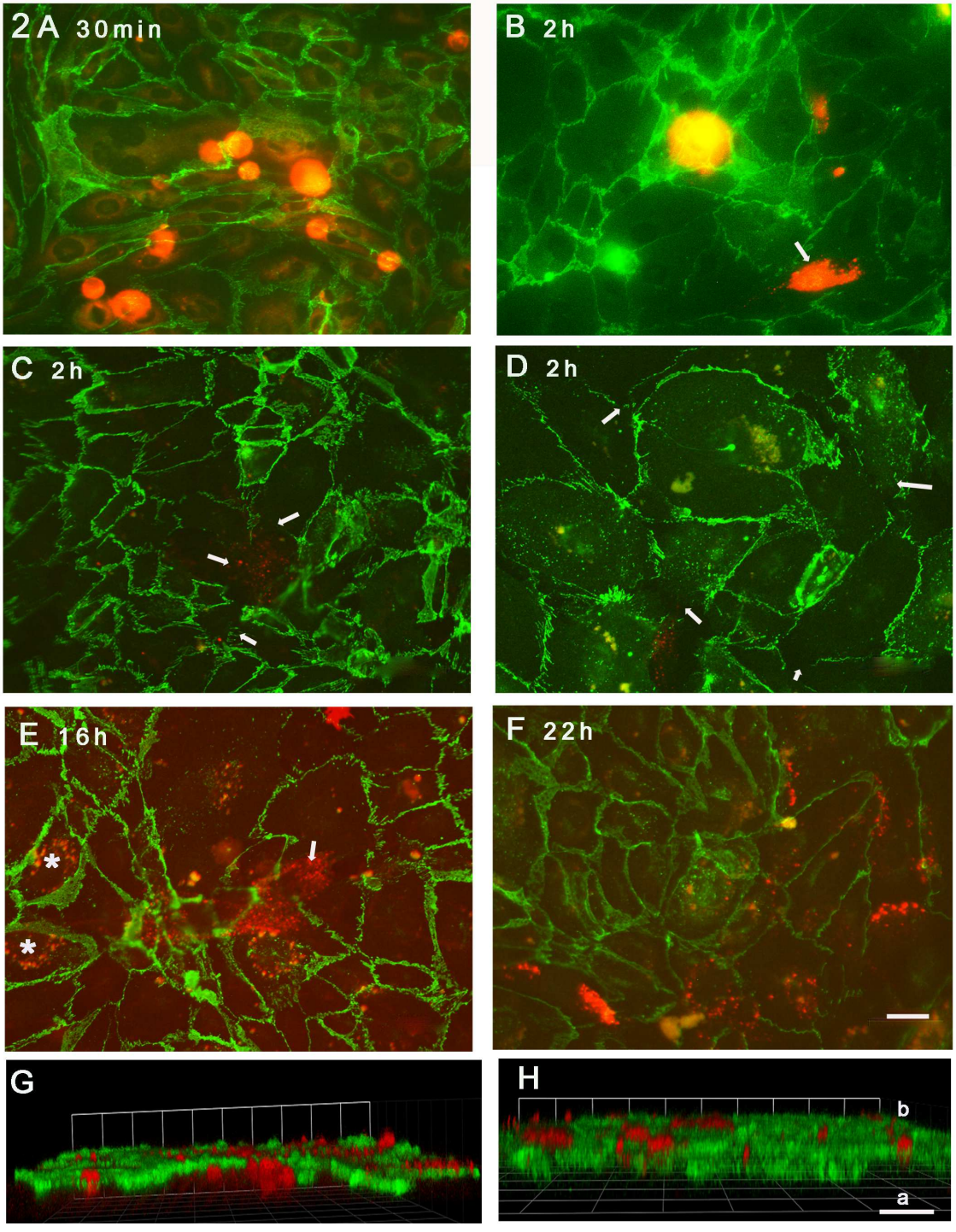
2A 30min
B 2h
C 2h
D 2h
E 16h
F 22h
G
H
b
a

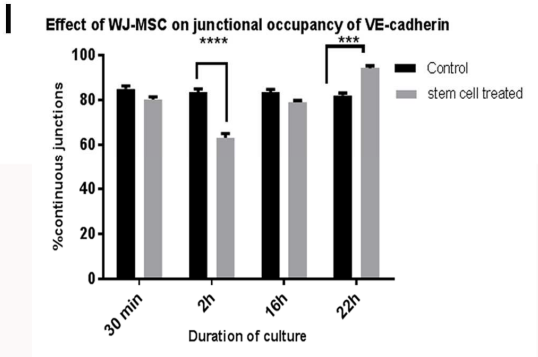
I
Effect of WJ-MSC on junctional occupancy of VE-cadherin
****
***
%continuous junctions
100
80
60
40
20
0
Control
stem cell treated
30 min
2h
16h
22h
Duration of culture

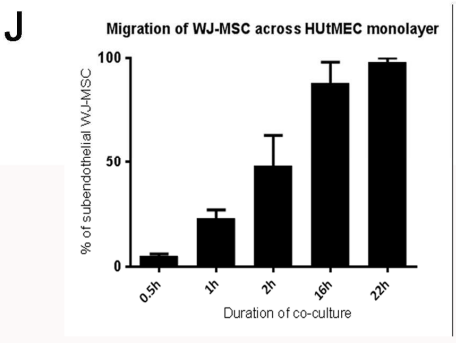
J
Migration of WJ-MSC across HUtMEC monolayer
% of subendothelial WJ-MSC
100
50
0
0.5h
1h
2h
16h
22h
Duration of co-culture

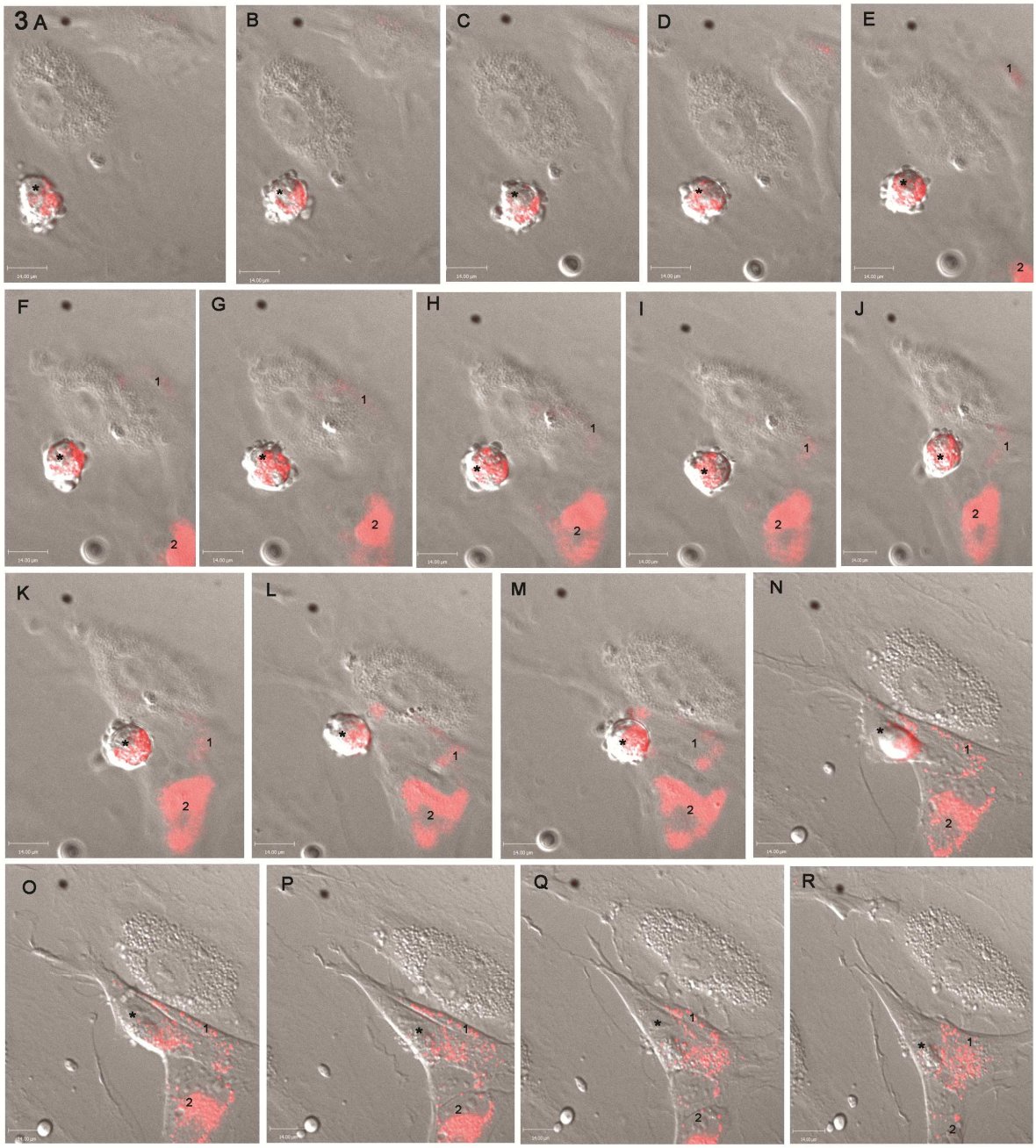
3A
B
C
D
E
F
G
H
I
J
K
L
M
N
O
P
Q
R
1
2
*

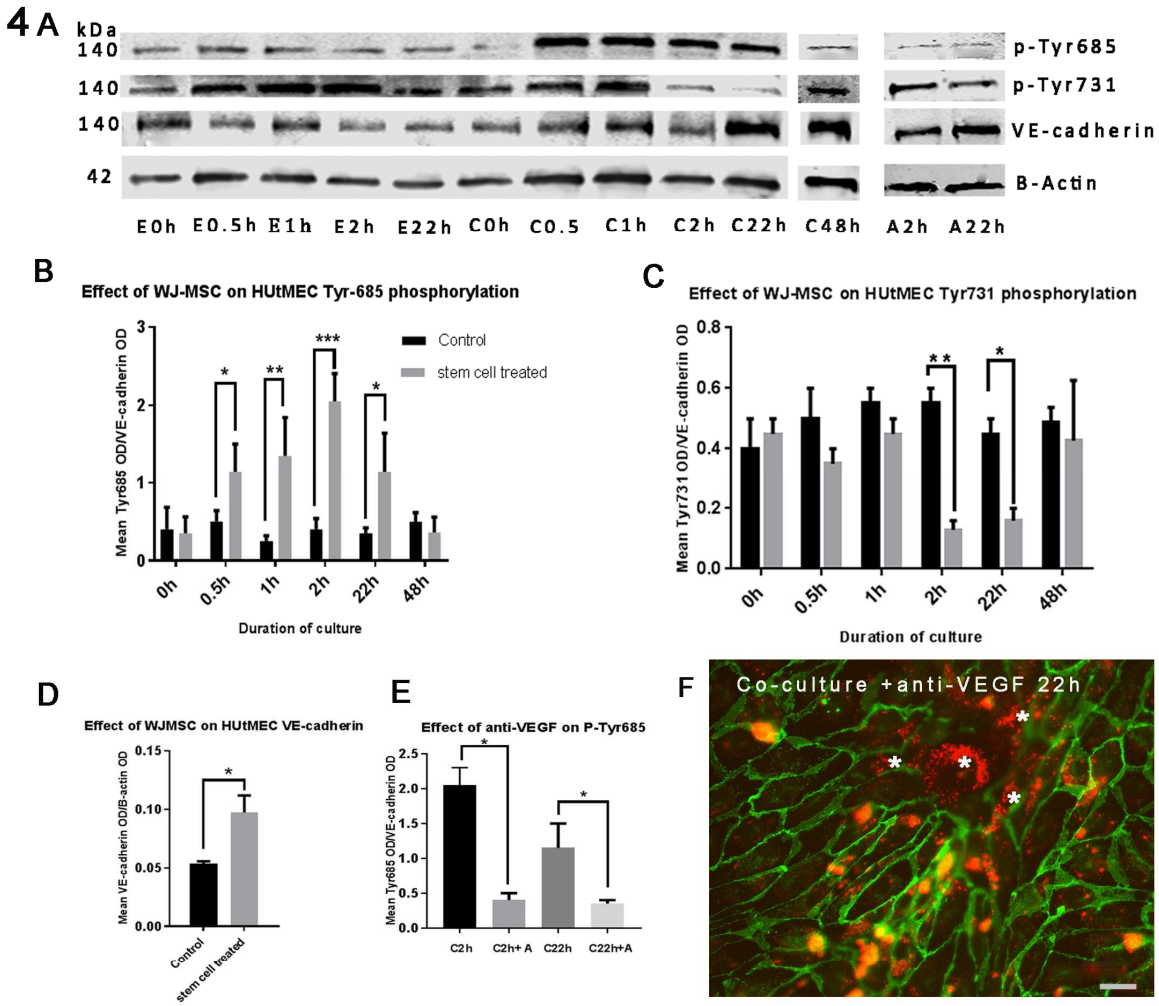
4 A
kDa
140
140
140
42
p-Tyr685
p-Tyr731
VE-cadherin
B-Actin
E0h E0.5h E1h E2h E22h C0h C0.5 C1h C2h C22h C48h A2h A22h
B
Effect of WJ-MSC on HUtMEC Tyr-685 phosphorylation
Mean Tyr685 OD/VE-cadherin OD
Control
stem cell treated
0h 0.5h 1h 2h 22h 48h
Duration of culture
C
Effect of WJ-MSC on HUtMEC Tyr731 phosphorylation
Mean Tyr731 OD/VE-cadherin OD
Duration of culture
D
Effect of WJMSC on HUtMEC VE-cadherin
Mean VE-cadherin OD/B-actin OD
Control
stem cell treated
E
Effect of anti-VEGF on P-Tyr685
Mean Tyr685 OD/VE-cadherin OD
C2h
C2h+ A
C22h
C22h+A
F
Co-culture +anti-VEGF 22h

5 A

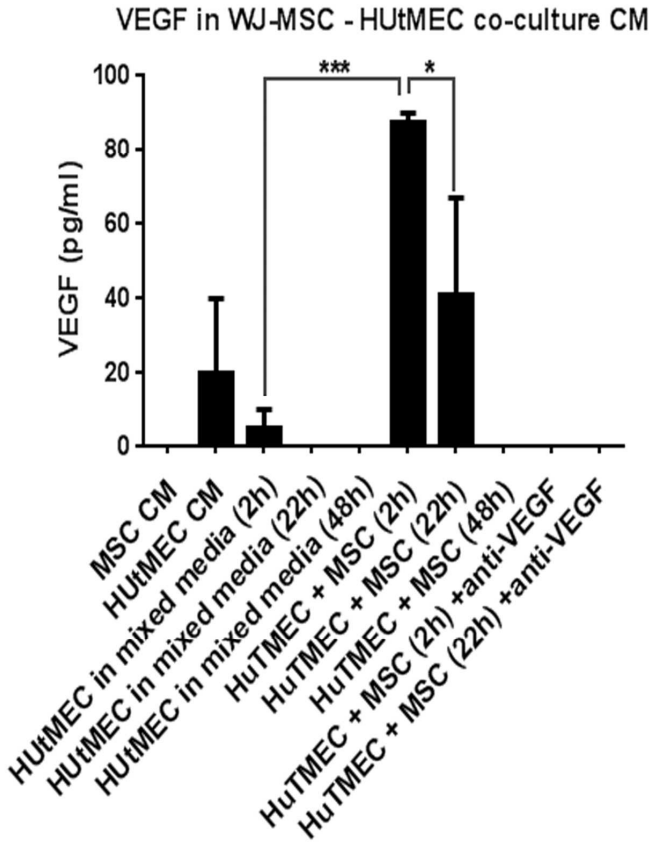
VEGF in WJ-MSC - HUtMEC co-culture CM
VEGF (pg/ml)
100
80
60
40
20
0
***
*
MSC CM
HUtMEC CM
HUtMEC in mixed media (2h)
HUtMEC in mixed media (22h)
HUtMEC in mixed media (48h)
HuTMEC + MSC (2h)
HuTMEC + MSC (22h)
HuTMEC + MSC (48h)
HuTMEC + MSC (2h) +anti-VEGF
HuTMEC + MSC (22h) +anti-VEGF

B

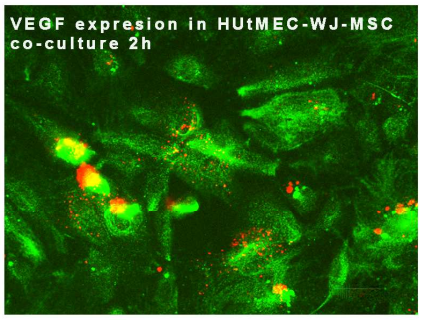
VEGF expresion in HUtMEC-WJ-MSC co-culture 2h

C

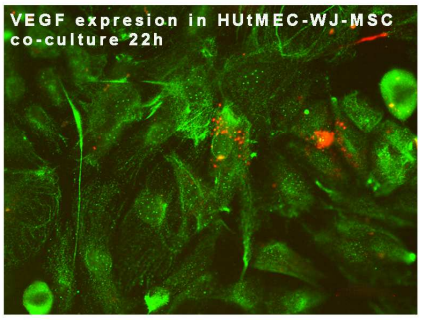
VEGF expresion in HUtMEC-WJ-MSC co-culture 22h

D

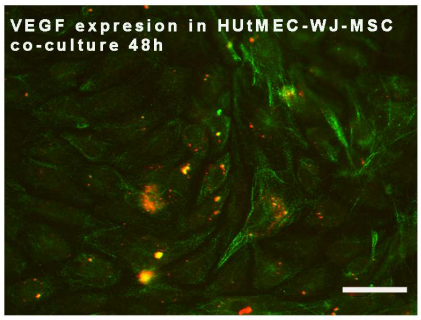
VEGF expresion in HUtMEC-WJ-MSC co-culture 48h

E

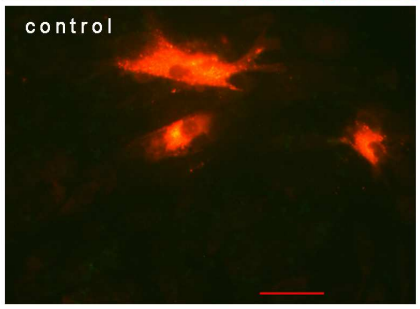
control

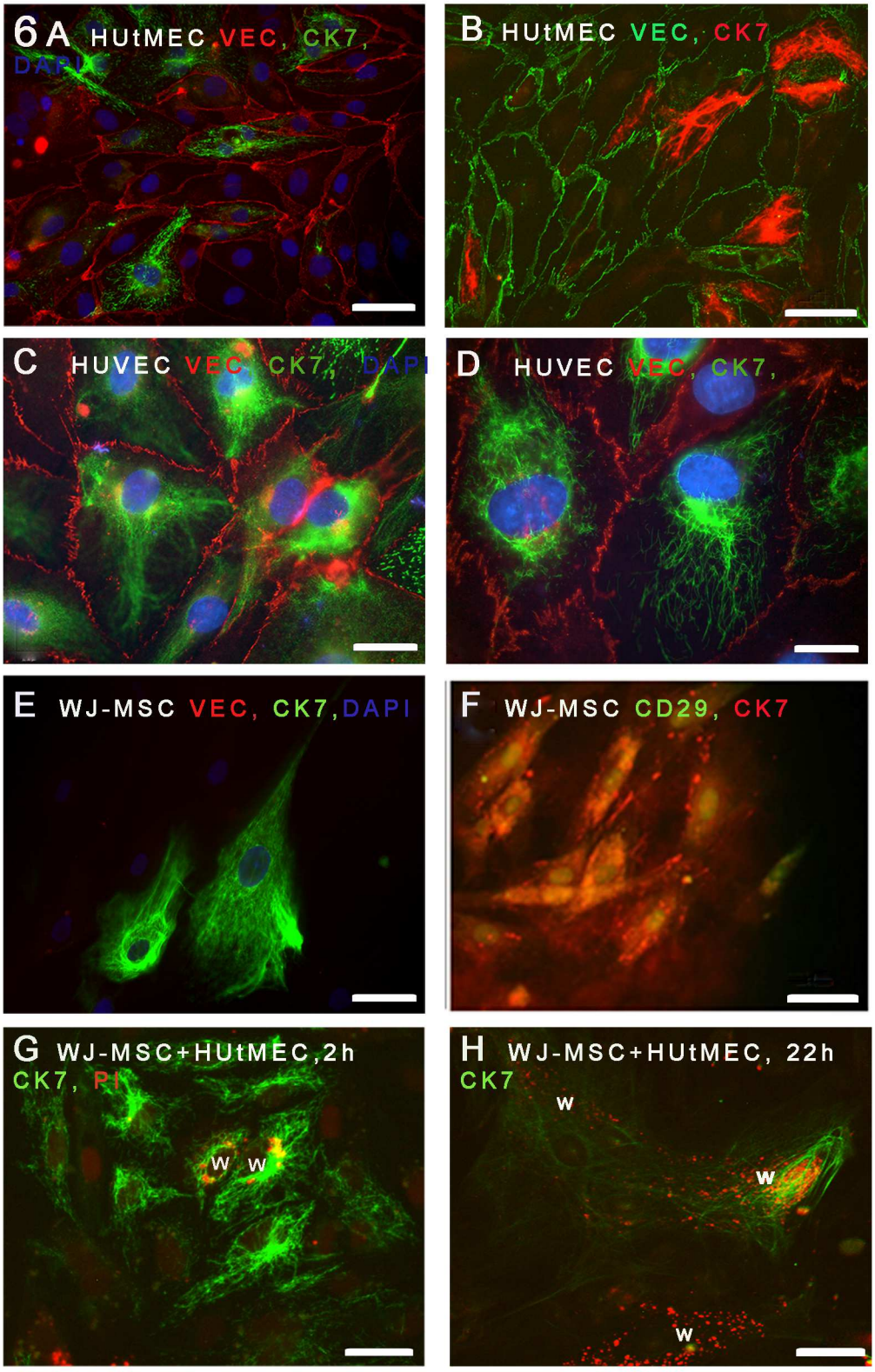
6 A HUtMEC VEC, CK7,
DAPI
B HUtMEC VEC, CK7
C HUVEC VEC, CK7, DAPI
D HUVEC VEC, CK7,
E WJ-MSC VEC, CK7, DAPI
F WJ-MSC CD29, CK7
G WJ-MSC+HUtMEC, 2h
CK7, PI
w w
H WJ-MSC+HUtMEC, 22h
CK7
w
w
w

Highlights

- WJ-MSC show non-destructive paracellular transmigration across uterine endothelial cells
- They alter VE-cadherin junctional occupancy to create frank paracellular gaps for extravasation
- Mechanisms include VEGF-dependent phosphorylation of Tyr685 and de-phosphorylation of Tyr731
- Re-sealing of junctions and upregulation of VE-cadherin occurs once WJ-MSC are sub-endothelial